Bioactive Materials 5 (2020) 659–666

Contents lists available at ScienceDirect

Bioactive Materials

journal homepage: http://www.keaipublishing.com/biomat

# Characteristics of novel Ti–10Mo-xCu alloy by powder metallurgy for potential biomedical implant applications

Wei Xu[a,b,e,1], Chenjin Hou[a,1], Yuxuan Mao[c], Lei Yang[c,**], Maryam Tamaddon[b], Jianliang Zhang[d], Xuanhui Qu[a], Chaozong Liu[b], Bo Su[e], Xin Lu[a,*]

[a] Beijing Advanced Innovation Center for Materials Genome Engineering, State Key Laboratory for Advanced Metals and Materials, Institute for Advanced Materials and Technology, University of Science and Technology Beijing, Beijing, China
[b] Institute of Orthopaedic & Musculoskeletal Science, University College London, Royal National Orthopaedic Hospital, Stanmore, HA7 4LP, UK
[c] Center for Health Science and Engineering, Tianjin Key Laboratory of Materials Laminating Fabrication and Interface Control Technology, School of Materials Science and Engineering, Hebei University of Technology, Tianjin, 300130, China
[d] School of Metallurgical and Ecological Engineering, University of Science and Technology Beijing, Beijing, 100083, China
[e] Bristol Dental School, University of Bristol, Bristol, BS1 2LY, UK

ARTICLE INFO

*Keywords:*
Ti-10Mo-xCu alloy
Microstructure
Mechanical properties
Cytocompatibility
Bacterial inhibitory property

ABSTRACT

When biomaterials are implanted in the human body, the surfaces of the implants become favorable sites for microbial adhesion and biofilm formation, causing peri-implant infection which frequently results in the failure of prosthetics and revision surgery. Ti–Mo alloy is one of the commonly used implant materials for load-bearing bone replacement, and the prevention of infection of Ti–Mo implants is therefore crucial. In this study, bacterial inhibitory copper (Cu) was added to Ti–Mo matrix to develop a novel Ti–Mo–Cu alloy with bacterial inhibitory property. The effects of Cu content on microstructure, tensile properties, cytocompatibility, and bacterial inhibitory ability of Ti–Mo–Cu alloy were systematically investigated. Results revealed that Ti–10Mo–1Cu alloy consisted of α and β phases, while there were a few $Ti_2Cu$ intermetallic compounds existed for Ti–10Mo–3Cu and Ti–10Mo–5Cu alloys, in addition to α and β phases. The tensile strength of Ti–10Mo-xCu alloy increased with Cu content while elongation decreased. Ti–10Mo–3Cu alloy exhibited an optimal tensile strength of 1098.1 MPa and elongation of 5.2%. Cytocompatibility study indicated that none of the Ti–10Mo-xCu alloys had a negative effect on MC3T3-E1 cell proliferation. Bacterial inhibitory rates against *S. aureus* and *E. coli* increased with the increase in Cu content of Ti–10Mo-xCu alloy, within the ranges of 20–60% and 15–50%, respectively. Taken together, this study suggests that Ti–10Mo–3Cu alloy with high strength, acceptable elongation, excellent cytocompatibility, and the bacterial inhibitory property is a promising candidate for biomedical implant applications.

## 1. Introduction

Titanium (Ti) and its alloys have received increasing attention in the field of orthopedics and dentistry, due to their excellent mechanical properties, corrosion resistance and biocompatibility [1–3]. However, the most widely used Ti and its alloys, e.g. commercial pure Ti (CP–Ti) and Ti–6Al–4V alloy (Ti64) (hereafter the composition of all alloys are given by wt.%), have some potential problems, including releasing toxic Aluminum (Al) or Vanadium (V) ions, stress-shielding because of the mismatch of elastic modulus between implant and bone, and bacterial infection [4,5]. Hence, many new β-type Ti alloys such as Ti–Nb–Zr and Ti–Mo based alloys have been designed and developed to enhance the biocompatibility and reduce the stress-shielding effect [6–9]. Among them, Ti–Mo based alloys with 4–20% Mo have attracted considerable attention due to their relatively low cost, high strength, low elastic modulus and excellent biocompatibility [10–15]. From the viewpoint of alloy design, less Mo is always preferred in the Ti–Mo alloys system because (1) Mo is expensive, minimizing the use of Mo reduces the cost; (2) Mo has a high melt pointing (2620 °C) than Ti (1660 °C), minimizing the use of Mo makes the Ti–Mo alloys easier to

Peer review under responsibility of KeAi Communications Co., Ltd.
* Corresponding author.
** Corresponding author.
*E-mail addresses:* ylei@hebut.edu.cn (L. Yang), luxin@ustb.edu.cn (X. Lu).
[1] These authors contributed equally.

https://doi.org/10.1016/j.bioactmat.2020.04.012
Received 25 March 2020; Received in revised form 15 April 2020; Accepted 16 April 2020

be processed. In addition, based on previous studies [16], 10% Mo is required in Ti–Mo alloys to retain the β-phase to make the alloy with a low elastic modulus. Therefore, the composition of Ti–10Mo is selected in this study.

On the other hand, bacterial infection is another major cause of Ti implants failure. It has been reported that even if surgery is operated under strict aseptic conditions, the average infection rate of orthopedic Ti implants is still as high as 0.5%–5% [17,18]. Therefore, developing Ti alloys with bacterial inhibitory properties is in urgent need. To date, there are mainly two approaches to enhance the bacterial inhibitory properties of Ti implants. One is the surface modification, e.g. ion implantation [19] and plasma immersion ion implantation (PIII) [20]. The other is to add bacterial inhibitory elements to Ti matrix, such as copper (Cu), silver (Ag), and zinc (Zn) [21–23]. Compared with surface modification, adding the bacterial inhibitory elements to the alloy matrix has many distinctive advantages, such as higher wear resistance and long-term bacterial inhibitory properties. Among bacterial inhibitory elements mentioned above, Cu has a low cost and cytotoxicity, and high antimicrobial efficiency. In addition, Cu is an essential element of several enzymes and a metabolizable agent [24], and is able to enhance vascularization and promote osteogenic differentiation and bone healing [25,26]. It was reported that some bacterial inhibitory metals have been successfully developed by adding Cu element into stainless steel, Ti and other metal alloys [27–30]. However, the effects of Cu on the comprehensive properties of Ti–Mo alloy are still scarce in the literature.

In the present study, Cu is added to Ti–10Mo alloy to develop novel β-type Ti alloys with low elastic modulus and bacterial inhibitory property. Given that the excessive Cu intake may result in cytotoxicity, 1–5 wt% Cu was added. The microstructure, tensile properties, cytocompatibility and bacterial inhibitory properties of Ti–10Mo-xCu alloy were investigated. The aims of this study were to systematically evaluate the newly developed Ti–10Mo-xCu alloy to support their potential applications in medical implants.

## 2. Materials and methods

### 2.1. Materials preparation

Commercially available Ti, Mo, and Cu powders (99.9% purity, Tian Tai Long Metal Materials Co., Ltd, China, and Beijing Xin Rong Yuan Co., Ltd, China) were used as raw materials. The chemical compositions of the powders are listed in Table 1. In order to decrease the oxygen content and hence enhance the mechanical properties, Ti powders were first coated by polyethylene glycol (PEG, Aladdin Shanghai Aladdin Bio-Chem Technology Co., Ltd, China). The amount of PEG was 1 wt% and the coating process is schematically shown in Fig. 1. The coated Ti, Mo and Cu powder with a nominal composition of Ti–10Mo-xCu (x = 0,1,3,5) were mixed in a blender for 6 h. Subsequently, the mixed powders were poured into a silicone mold and compacted by cold isostatic pressing (CIP) at 200 MPa. Finally, the green compacts were sintered at different temperatures in the range of 1300–1420 °C in a tube furnace under an argon atmosphere. The PEG, which boiling point was about 250 °C, was decomposed and volatilized completely during sintering. The O content of Ti, Mo, and Cu powders was below 0.15 wt %, and the particle size of all powders was ≤45 μm. The detailed information of impurity contents and particle size of the powders were described elsewhere [31,32].

**Table 1**
Chemical composition of Ti, Mo and Cu powders.

| Powder | Chemical composition (wt.%) | | | | | | | | | |
|---|---|---|---|---|---|---|---|---|---|---|
| | H | C | N | O | Si | Cl | Fe | Cu | Ti | Mo |
| Ti | 0.03 | 0.02 | 0.04 | 0.15 | 0.02 | 0.05 | 0.02 | 0 | Bal. | 0 |
| Mo | 0.07 | 0.05 | 0.05 | 0.20 | 0.02 | 0.01 | 0.02 | 0 | 0 | Bal. |
| Cu | 0.03 | – | – | 0.02 | – | 0.04 | 0.01 | Bal. | 0 | 0 |

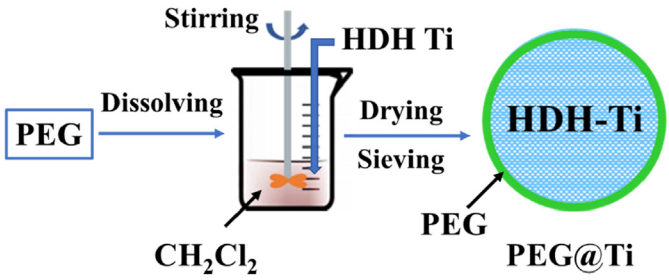


**Fig. 1.** Schematic illustration of the coating process of Ti powder with PEG.

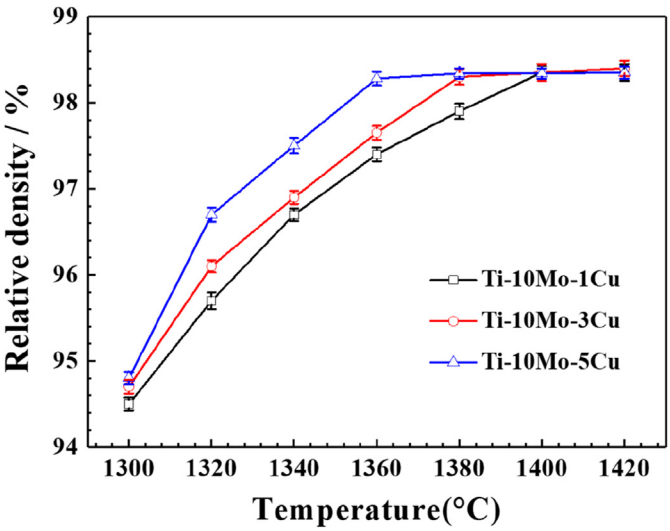


**Fig. 2.** Influence of sintering temperature and Cu contents on the relative density of Ti–10Mo-xCu alloy.

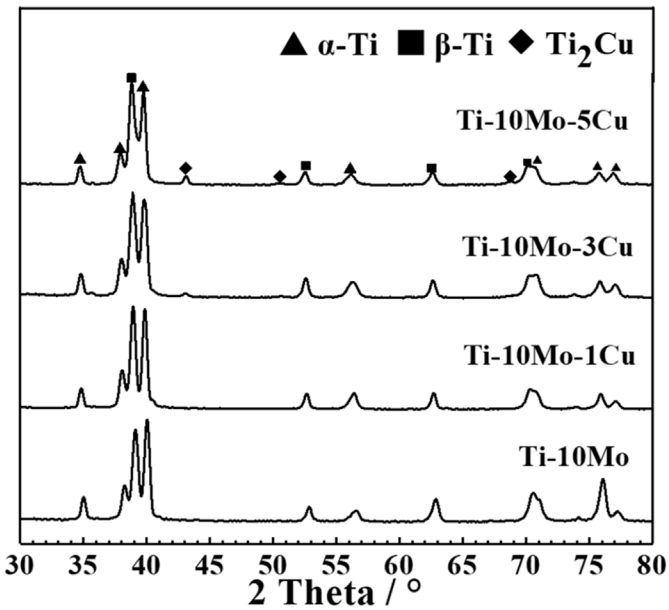


**Fig. 3.** XRD patterns of Ti–10Mo-xCu alloy with different Cu contents.

### 2.2. Microstructure characterization

The Archimedes method was used to measure the density of sintered

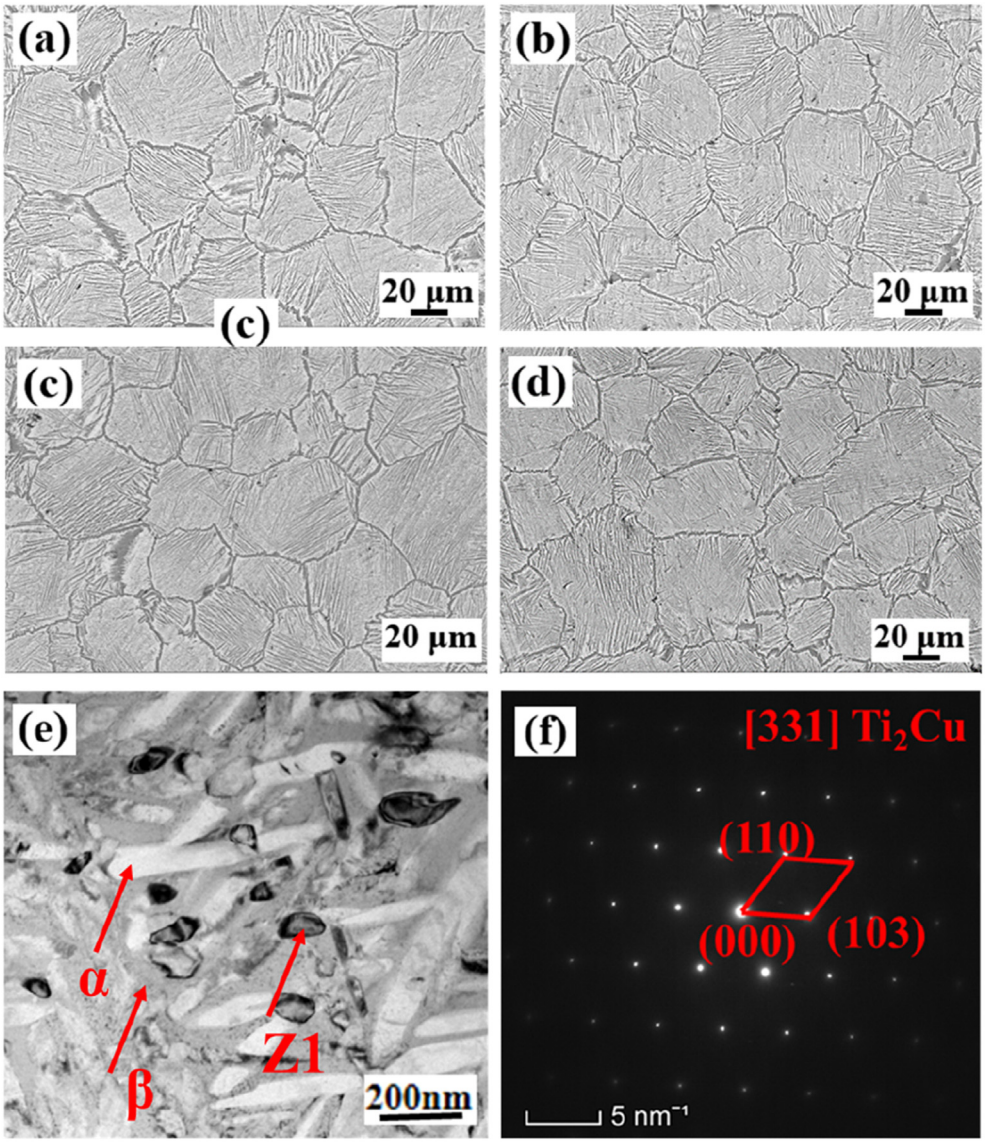


**Fig. 4.** Microstructure of Ti–10Mo-xCu alloy with different Cu contents: (a) Ti–10Mo; (b) Ti–10Mo–1Cu; (c) Ti–10Mo–3Cu; (d) Ti–10Mo–5Cu; (e) Morphology of $Ti_2Cu$ phase in Ti–10Mo–5Cu alloy; (f) Corresponding selected area diffraction pattern of the area Z1 in (e).

specimens based on the ASTM B962-14 (2017) standard [33]. The phase constituent and microstructure of the specimens were characterized using an X-ray diffractometer (Rigaku, Japan), scanning electron microscope (SEM, JSM-6480LV, Japan), and transmission electron microscopy (TEM, Tecnai G2 F20, USA). The target of the X-ray diffractometer was Copper (Cu) while the wavelength was 0.15406 nm. The voltage and electric current for X-ray diffractometer are 40 kV and 50 mA, respectively. The scanning speed is 10°/min, and the scanning angle is in the range of 20°–90°. Before the microstructural analysis using SEM, all specimens were ground with SiC abrasive paper to 2000#, polished, and then etched using Kroll's etchant. The Kroll's etchant consists of hydrofluoric acid, nitric acid, and distilled water, and the volume ratio is 5:10:85. The TEM specimens were prepared using a focused ion beam (FIB, Helios nanolab600i, USA).

### 2.3. Mechanical testing

The tensile property of Ti–10Mo-xCu alloy was tested by an INSTRON 4206 machine under a strain rate of 0.002 $s^{-1}$. The diameter and gauge length of specimens were 3 mm and 15 mm, respectively. The tensile strength and elastic modulus were calculated from the engineering stress-strain curves, and the fractured surface was observed by SEM.

### 2.4. Cytocompatibility testing

Murine osteoblast cells (MC3T3-E1) obtained from cell bank from the Chinese academy of sciences was adopted to evaluate the cytocompatibility of Ti–10Mo-xCu alloy. MC3T3-E1 cells were seeded in 24-well plates containing sterilized Ti–10Mo-xCu alloy, and initial density was $1 \times 10^5$ cells/well. Then the plates were cultured at 37 °C with 5% $CO_2$. At day 1 and day 3, the culture medium was discarded and 20 μL Cell Counting Kit-8 (CCK-8, Sigma) solution was added into each well, and cultured for another 4 h. Finally, the absorbance of each well was measured on a Bio-Rad microplate reader at 570 nm. The cell relative growth rate (CRGR) was calculated based on the following formula:

$$CRGR = (OD_{570nm}\ \text{specimen}/OD_{570nm}\ \text{blank}) \times 100\% \quad (1)$$

where $OD_{570nm}$ specimens and $OD_{570nm}$ blank are the optical density of the Ti-10-xCu specimens and blank controls, respectively. Based on the International Standard ISO 10993–5 [34], the cytotoxic level was categorized into six groups: 0 ≥ 100%; I: 75%–99%; II: 50%–74%; III: 25

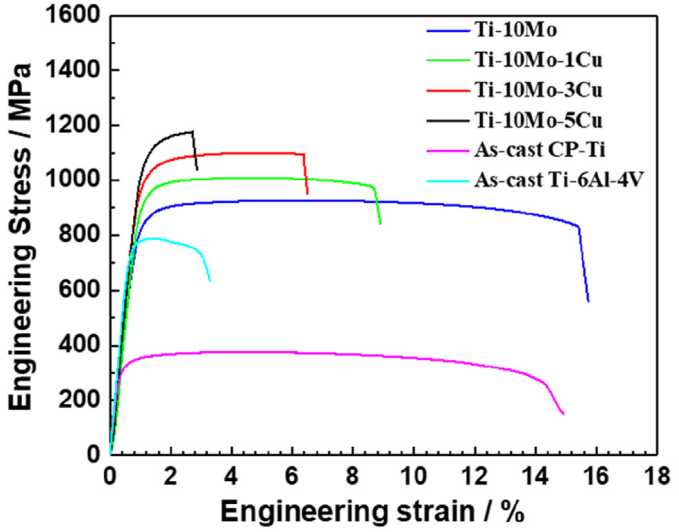


**Fig. 5.** Tensile stress-strain curves of Ti–10Mo-xCu alloy with different Cu contents.

%-49%; IV: 1%–24%; V: ≤1%. In addition, the live and dead cells were stained by a LIVE/DEAD kit (Thermo Fisher Scientific) at days 1 and 3. The procedure was as follows: (1) the medium was removed; (2) 4 μM calcein-AM and 2 μM ethidium homodimer-1 in phosphate-buffered saline (PBS) solution was added; (3) the plate was incubated in the dark for 15 min at 37 °C; (4) the cells were observed by a confocal laser scanning microscope (Zeiss 880, Germany).

### 2.5. Bacterial inhibitory test

In order to evaluate the bacterial inhibitory properties of Ti–10Mo-xCu alloy, *Staphylococcus aureus* (*S. aureus*) and *Escherichia coli* (*E. coli*) strains were cultured with the alloys. Before culturing, all specimens were sterilized with UV irradiation for 1 h. The diameter and thickness of the specimens were 8 mm and 0.5 mm, respectively. Ti–10Mo alloy was used as a control. Before experiments, the *S. aureus* and *E. coli* were cultured in an NB (nutrient broth) at 37 °C to a concentration of $10^6$ CFU/mL. Then it was diluted to a concentration of $10^5$ CFU/mL by PBS solution. 50 μL diluted bacteria suspension was added to the 24-well plate to co-culture with the specimens for 24 h at 37 °C. After 24 h culturing, the plate-count method was used to calculate the number of bacterial based on the GB/T 2591 standard [35]. The bacterial inhibitory rate (R) was calculated based on the following formula:

$$R = (N_{reference} - N_{specimen}) / N_{reference} \times 100\% \quad (2)$$

Where $N_{reference}$ and $N_{specimen}$ are the numbers of the bacterial colonies on Ti–10Mo and Ti-10-xCu specimens, respectively.

### 2.6. Cu ion release

Ti–10Mo-xCu alloys were immersed in the deionized water at a ratio of 3 $cm^2$/ml (the surface area of the disc to the volume of media) to examine the Cu ion release. After day 1, 3, 5, and 7, ICP-MS (inductively coupled plasma mass spectrometry, PerkinElmer, Optima 5300 DV) method was used to evaluate the Cu ion concentration. Five tests were repeated at each time, and the average value was reported.

### 2.7. Statistical analysis

All the tests were performed in triplicate. Results of mechanical, cytocompatibility, bacterial inhibitory, and Cu ion release tests are expressed as means ± standard deviations. The differences between groups were observed by one-way analysis of variance (SPSS 14.0 for Windows, SPSS Inc., Chicago, IL) to determine the statistical significance. $P < 0.05$ was considered statistically significant.

## 3. Results and discussion

### 3.1. Density and microstructure

Fig. 2 shows the variation in the relative density of specimens as a function of sintering temperature and Cu contents. The relative density strongly depends on the sintering temperature and Cu contents. Generally, the relative density increases gradually and then tends to stabilize at a certain level (about 98%) with the increasing sintering temperature at the same Cu content. In addition, the relative density increases with Cu content at the same sintering temperature, and the minimum sintering densification temperature decreases gradually with Cu content. This is mainly because Cu (melting point 1083.4 °C) is a low-melting metal compared with Ti (melting point 1660.0 °C) and Mo (melting point 2620 °C). Thus, with increasing Cu content, the melting pointing of the alloys decreases and the corresponding minimum sintering densification temperature also decreases. For the Ti–10Mo–1Cu, Ti–10Mo–3Cu, Ti–10Mo–5Cu alloys, the minimum sintering densification temperature is 1400 °C, 1380 °C, and 1360 °C, respectively, and the relative density is in the range of 98.12%–98.35%.

Fig. 3 shows the XRD patterns of Ti–10Mo-xCu alloy with different Cu contents. It can be seen that all the Ti–10Mo-xCu alloy mainly consists of α and β phases. For the Ti–10Mo–3Cu and Ti–10Mo–5Cu alloy, there is also a small amount of $Ti_2Cu$ phase, which increases with the Cu content increase. This result agrees with the previous results reported by Campo [36].

The SEM images of Ti–10Mo-xCu alloy and TEM images with the

**Table 2**
Tensile properties of Ti–10Mo-xCu alloy with different Cu contents and common Cu-bearing Ti alloys.

| Materials | Preparation | UTS/MPa | El./% | E/GPa | |
|---|---|---|---|---|---|
| Ti–10Mo | PM | 916.2 ± 11.2 | 14.8 ± 0.3 | 77.6 ± 1.3 | This study |
| Ti–10Mo–1Cu | PM | 1002.3 ± 12.2 | 8.2 ± 0.1 | 73.5 ± 1.6 | This study |
| Ti–10Mo–3Cu | PM | 1098.1 ± 9.4 | 5.2 ± 0.2 | 71.1 ± 0.9 | This study |
| Ti–10Mo–5Cu | PM | 1162.2 ± 13.6 | 1.97 ± 0.2 | 74.9 ± 1.5 | This study |
| CP-Ti | Casting | 375.1 ± 5.4 | 14.1 ± 0.4 | 106.1 ± 2.1 | This study |
| Ti–6Al–4V | Casting | 788.1 ± 9.1 | 2.53 ± 0.1 | 110.2 ± 1.8 | This study |
| Ti–5Cu | Casting | 535 | 14.5 | – | [37] |
| Ti–6Al–4V–1Cu | Casting | 1016 | 2.8 | 99 | [38] |
| Ti–6Al–4V–4Cu | Casting | 884 | 1.0 | 88 | [38] |
| Ti–6Al–4V–10Cu | Casting | 387 | 0.2 | 162 | [38] |
| Ti–3Cu | Annealing (740 °C) | 575 | 21 | – | [39] |
| Ti–5Cu | Annealing (740 °C) | 594 | 26 | – | [39] |
| Ti–7Cu | Annealing (740 °C) | 649 | 23 | – | [39] |
| Ti–3Cu | Annealing (830 °C) | 584 | 24 | – | [39] |

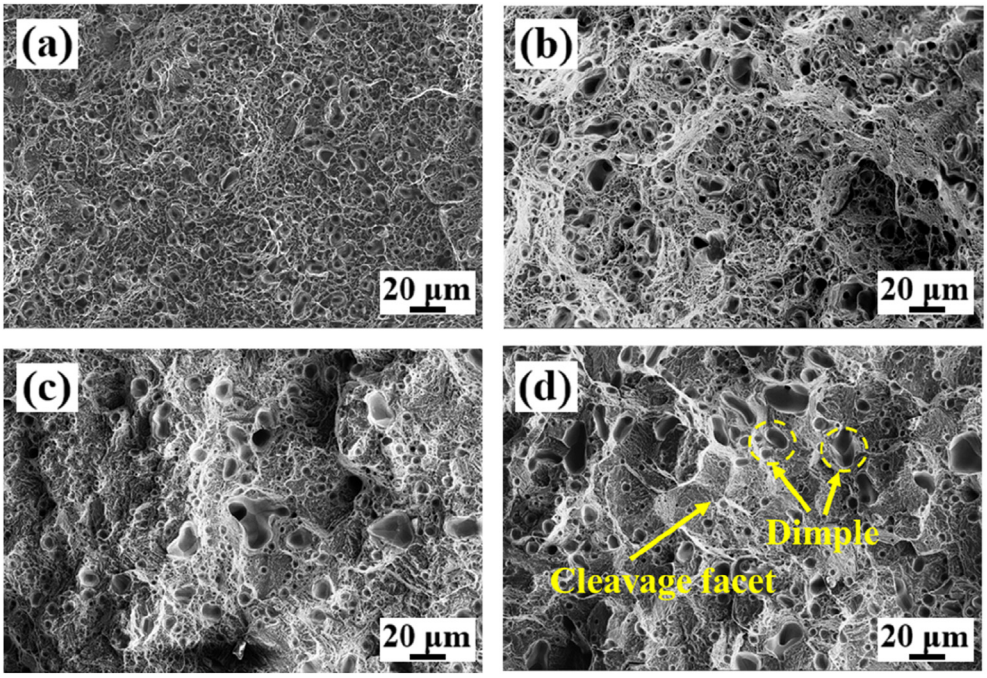


**Fig. 6.** SEM images of tensile fracture surfaces of Ti–10Mo-xCu alloy with different Cu contents: (a) Ti–10Mo; (b) Ti–10Mo–1Cu; (c) Ti–10Mo–3Cu; (d) Ti–10Mo–5Cu.

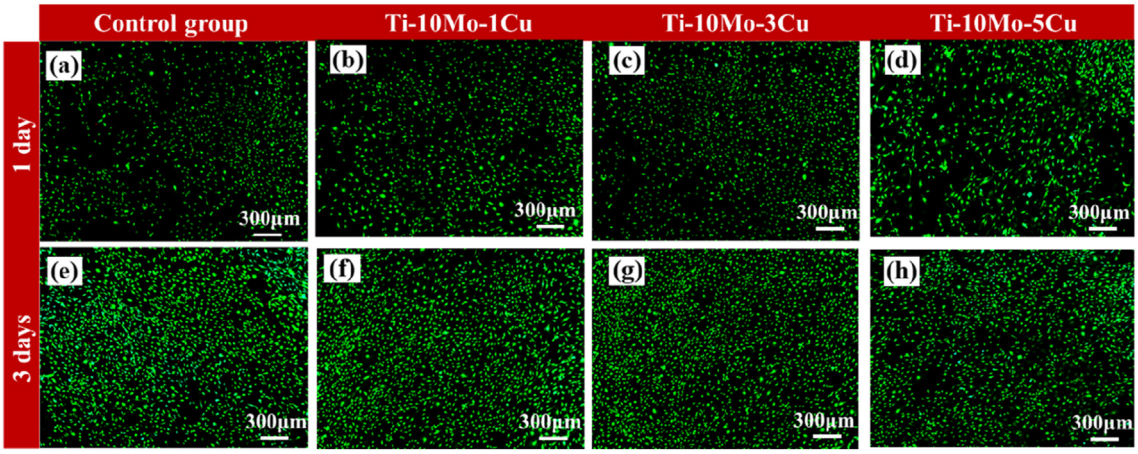


**Fig. 7.** Merged images of live and dead cells on Ti–10Mo-xCu alloy of different Cu contents after culturing for different days.

corresponding selected area diffraction patterns of Ti–10Mo–5Cu alloys are shown in Fig. 4. As Fig. 4 (a)–(d) show, Ti–10Mo-xCu alloy with high relative density can be obtained by the PM method, which is consistent with the densification result (Fig. 2). All specimens exhibit a uniform Widmanstätten structure, which consists of α and β phases. Though the $Ti_2Cu$ phase exists in XRD for Ti–10Mo–3Cu and Ti–10Mo–5Cu alloys, it is not observed in SEM. This may be because the size of $Ti_2Cu$ is too small to be distinguished. To confirm the existence of the $Ti_2Cu$ phase, the microstructure of Ti–10Mo–5Cu alloy is characterized using TEM, as shown in Fig. 4(e). It can be seen that there were some dark particles (marked as Z1) in the size range of 80–150 nm. The EDS analysis revealed that the area Z1 consisted of Ti and Cu with an atomic percentage of 68.72 and 31.28. The corresponding selected area diffraction pattern of the area Z1 is shown in Fig. 4(f). The EDS results together with the corresponding selected area diffraction pattern confirmed that the dark particle is the $Ti_2Cu$ phase.

### 3.2. Mechanical properties

The typical engineering stress-strain curves of Ti–10Mo-xCu alloy with different Cu content, together with as-cast CP-Ti and Ti64 alloys as controls, are presented in Fig. 5. It can be seen that the tensile strength of Ti–10Mo-xCu alloy increases with the rise in the Cu content while the elongation decreases gradually. All Ti–10Mo-xCu alloy exhibit higher tensile strength than as-cast CP Ti and Ti64 alloys.

The mechanical properties of the PM-fabricated Ti–10Mo-xCu alloy with different Cu content are summarized in Table 2, and compared with common Cu-bearing Ti alloys, including Ti–Cu and Ti–6Al–4V–Cu alloys. It can be seen that the tensile strength of Ti–10Mo-xCu alloy is in the range of 916.2–1162.2 MPa while the elongation decreases from 14.8 to 1.97. This is mainly because of the existence of the $Ti_2Cu$ phase and solid solution strengthening of Cu. With a higher Cu content, the solid solution strengthening effect is gradually enhanced, which leads to increased strength. In addition, it is well known that $Ti_2Cu$ is an intermetallic, which is a hard-brittle phase. It usually enhances strength while reducing elongation. With the increase in Cu content, the

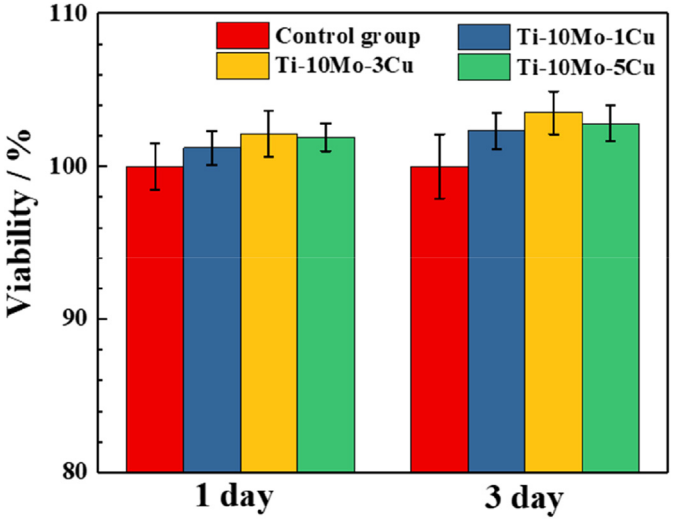


**Fig. 8.** Viability of MC3T3-E1 cells cultured on Ti–10Mo-xCu alloy of different Cu contents.

Ti–10Mo-xCu alloy presents higher $Ti_2Cu$ content (Fig. 3). As a result, the strength of the Ti–10Mo-xCu alloy increases while the elongation decreases gradually. Successful clinical application of the metal alloy depends largely on meeting the requirements of mechanical properties, namely a high strength and an elongation not less than 5%. Hence, the Ti–10Mo–3Cu alloy with an optimal property with high strength of 1098.1 MPa and an acceptable elongation of 5.2% is a promising material for medical implant. Compared with the Cu-bearing Ti alloys in the literature, such as Ti–6Al–4V-xCu and Ti-xCu alloys, Ti–10Mo–3Cu alloy exhibits higher tensile strength with an elongation lower than Ti-xCu alloy (14.5%–26%) but higher values than Ti–6Al–4V-xCu (0.2%–2.8%).

The microscopic fracture morphologies of Ti–10Mo-xCu alloy with different Cu contents are shown in Fig. 6. Fewer pores are observed for all alloys, owing to its near full density (relative density is above 98%, Fig. 2). In addition, the fracture surfaces of all alloy display mixture of dimples of varying size and coarse cleavage facet, which demonstrates that the fracture mode of the Ti–10Mo-xCu alloy is a quasi-cleavage fracture. But the size of the dimples become larger while the number decreases, while the amount of cleavage surface increases with the rise in Cu content. This result indicates that the strength of the alloys increases and the elongation decreases with Cu content, which is in good agreement with the tensile stress-strain curves.

### 3.3. Cytocompatibility

In order to investigate the potential application of Ti–10Mo-xCu alloy for bone implants, MC3T3-E1 cells were used to evaluate the cytocompatibility. In this study, the viability of the MC3T3-E1 cells cultured on the surface of alloys after 1 and 3 days is evaluated using a LIVE/DEAD kit. The merged live and dead images are shown in Fig. 7. It can be seen that there are a few dead cells (fluorescent red) observed and most of the cells are viable (bright fluorescent green) for all of the alloys at day 1. With the prolongation of culture time to 3 days, there are more viable cells on the surface of the alloys. In addition, there is no significant difference in viable cells observed among the Ti–10Mo-xCu alloy and control group, which indicates that the cells could proliferate on all the newly developed Ti–10Mo-xCu alloy.

In order to qualify the proliferation of MC3T3-E1 cells on Ti–10Mo-xCu alloy, CCK8 assay tests were carried out, and the cell CRGR is calculated based on formula (1), and the results are shown in Fig. 8. It can be seen that with the increasing culture time, cell proliferation increases on all specimens. The CRGR of all alloys is higher than 100% after 1 and 3 days. Based on ISO 10993–5 [34], the cytotoxicity level for all Ti–10Mo-xCu alloy is categorized level 0. This result together with the live and dead staining results indicates that none of the Ti–10Mo-xCu alloys are cytotoxic to MC3T3-E1 cells.

### 3.4. Bacterial inhibitory property

Fig. 9 shows the CFU of *E. coli* and *S. aureus* bacteria cultured on the surface of Ti–10Mo-xCu alloy and Ti–10Mo alloy (as control) after 24 h. The CFU results suggest that there are large amounts of *E. coli* and *S. aureus* grew on the surface of Ti–10Mo alloy compared with the Ti–10Mo-xCu alloy after 24 h incubation. The CFU numbers of *S. aureus* and *E. coli* colonies from Ti–10Mo-xCu alloy groups decrease with the increase in Cu content. The calculated bacterial rate is shown in Table 3. It can be seen that the bacterial inhibitory rates of Ti–10Mo-xCu alloy increase with the Cu content after 24 h incubation. The bacterial inhibitory rates of Ti–10Mo-xCu alloy against *S. aureus* are about 20%, 40%, and 60%, respectively, while that against *E. coli* is about 15%, 35%, and 50%.

The Cu ion release in the deionized water with the immersion time is shown in Fig. 10. It can be seen that a relatively high Cu ion concentration is released from all Ti–10Mo-xCu alloy. In general, the amount of Cu ion release increases linearly with the Cu content at the same timepoint. The release amount at the first day for Ti–10Mo-xCu alloy was in the range of 0.06–0.09 mg/L, which increases continually with prolonged immersion time. After 7 days, the amount of released

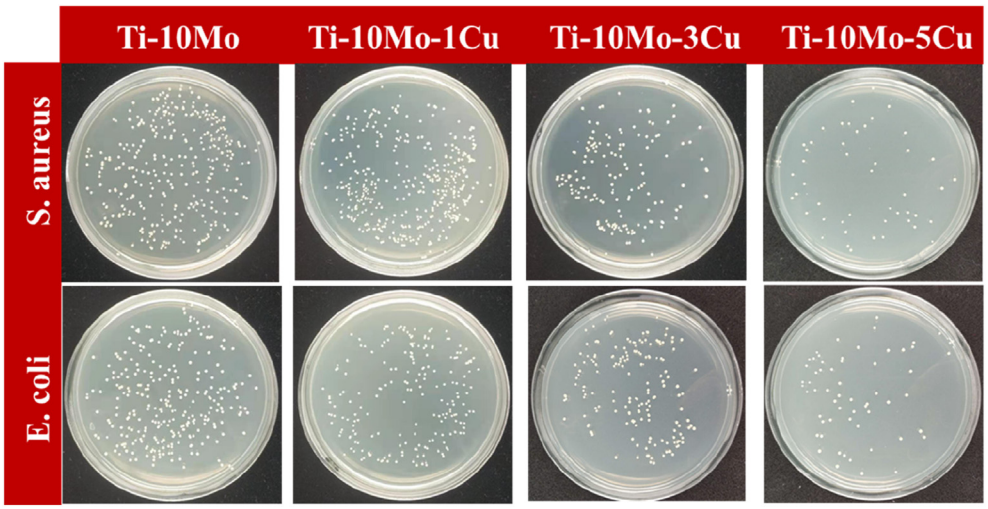


**Fig. 9.** *Staphylococcus aureus* and *Escherichia coli* bacterial colonies after incubation for 24 h on Ti–10Mo-xCu alloy with different Cu contents.

**Table 3**
Bacterial inhibitory rate of Ti–10Mo-xCu alloy with different Cu contents.

| Alloy | *Staphylococcus aureus* number (CFU × $10^7$) | *Staphylococcus aureus* inhibition rate (%) | *Escherichia coli* number (CFU × $10^7$) | *Escherichia coli* bacterial inhibition rate (%) |
|---|---|---|---|---|
| Ti–10Mo | 4.11 | – | 6.17 | – |
| Ti–10Mo–1Cu | 3.19 | 22.4 | 5.16 | 16.4 |
| Ti–10Mo–3Cu | 2.39 | 41.8 | 3.93 | 36.3 |
| Ti–10Mo–5Cu | 1.59 | 61.3 | 3.01 | 49.9 |

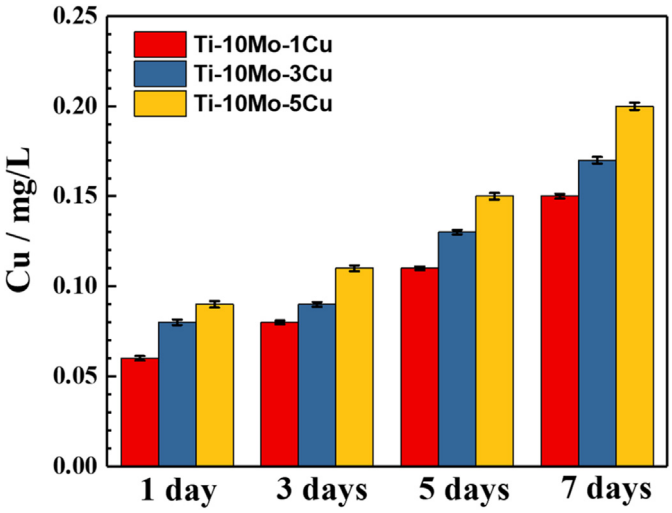


**Fig. 10.** The cumulative Cu ion concentration in the deionized water with the immersion time.

Cu ion for Ti–10Mo–1Cu, Ti–10Mo–3Cu, and Ti–10Mo–5Cu alloy are 0.15 mg/L, 0.17 mg/L, and 0.20 mg/L, respectively.

The enhanced bacterial inhibitory properties of Ti–10Mo-xCu alloy can be ascribed to the following factors: (1) the release of Cu ion; and (2) the existence of the $Ti_2Cu$ phase. It has been suggested that Cu is a broad bacterial inhibitory agent, mainly as a result of releasing Cu ion. As shown in Fig. 8, the amount of releasing $Cu^{2+}$ increases gradually with the Cu content and time, meaning that it can sustainably kill bacteria. In addition to the $Cu^{2+}$, $Ti_2Cu$ also plays an important role in killing bacteria. Base on previous studies [40], fine and dispersed $Ti_2Cu$ phase could lead to a higher bacterial inhibitory rate. In this study, with the Cu content increases, the release of Cu ion and the amount of the $Ti_2Cu$ phase increase simultaneously, which leads to a gradual increase in the bacterial inhibitory rate. However, compared with other Ti alloys with the same Cu content [37–42], e.g. Ti-xCu and Ti–6Al–4V-xCu alloys, the bacterial inhibitory rate of Ti–10Mo-xCu alloy is still relatively low. This might be caused by a different bacterial inhibitory mechanism, and the detailed bacterial inhibitory mechanism needs to be explored in the future. Based on the above results, the Ti–10Mo–3Cu alloy exhibits higher strength, excellent cytocompatibility, and comparable elongation and bacterial inhibitory properties, and it could be considered as a promising candidate for bone-tissue engineering application.

## 4. Conclusions

New Ti–10Mo-xCu alloy with the bacterial inhibitory effect is developed and fabricated from a PM route in this study. The microstructure, mechanical properties, cytocompatibility, and bacterial inhibitory property of the Ti–10Mo-xCu alloy are fully characterized. The main conclusions are summarized as follows:

(1) Ti–10Mo-xCu alloy with a high relative density (about 98%) is successfully fabricated by simple PM. All Ti–10Mo-xCu alloy shows a typical Widmanstäten microstructure. Ti–10Mo–3Cu and Ti–10Mo–5Cu alloys also have a small amount of $Ti_2Cu$ phases.
(2) A wide range of mechanical properties of Ti–10Mo-xCu alloy can be achieved. The Ti–10Mo–3Cu alloy exhibits an optimal tensile strength of 1098.1 MPa and elongation of 5.2%.
(3) No adverse effects of the Ti–10Mo-xCu alloy generated on the MC3T3-E1 cell proliferation, and the cytotoxicity level is extremely low (grade 0). With the increase in Cu content, the bacterial inhibitory rates of Ti–10Mo-xCu alloy increase gradually, and the rates against *S. aureus* and *E. coli* are in the range of 20–60% and 15–50% after 24 h incubation, respectively.
(4) Ti–10Mo–3Cu alloy exhibits high strength, excellent cytocompatibility, good elongation and bacterial inhibitory property, and therefore can be considered for further study as a medical implant material.

## Data availability

The data that support the findings of this study are available from the corresponding authors on reasonable request.

## CRediT authorship contribution statement

**Wei Xu:** Conceptualization, Data curation, Formal analysis, Writing - original draft, Writing - review & editing. **Chenjin Hou:** Data curation, Formal analysis, Investigation. **Yuxuan Mao:** Investigation, Writing - review & editing. **Lei Yang:** Investigation, Writing - review & editing. **Maryam Tamaddon:** Investigation, Writing - review & editing. **Jianliang Zhang:** Investigation, Writing - review & editing. **Xuanhui Qu:** Formal analysis, Investigation. **Chaozong Liu:** Formal analysis, Investigation. **Bo Su:** Investigation, Writing - review & editing. **Xin Lu:** Conceptualization, Supervision, Project administration.

## Declaration of competing interest

The authors declare that they have no known competing for financial interests or personal relationships that could have appeared to influence the work reported in this paper.

## Acknowledgments

This research work is supported by the National Natural Science Foundation of China (51922004, 51874037, 51672184), State Key Lab of Advanced Metals and Materials, University of Science and Technology Beijing (2019-Z14) and Fundamental Research Funds for the Central Universities (FRF-TP-19005C1Z). Chaozong Liu acknowledges the support from the European Commission via the H2020 MSCA RISE BAMOS programme (734156). Bo Su would like to thank financial support from the MRC (MR/S010343/1) and the EU H2020 MSCA RISE Bio-TUNE programme. Wei Xu acknowledges the support from the China Scholarship Council (CSC) for a CSC Ph.D. scholarship (201906460106).

## References


[1] A. Nouri, C. Wen, 1-Introduction to Surface Coating and Modification for Metallic Biomaterials, Surface Coating and Modification of Metallic Biomaterials, Woodhead Publishing, 2015, pp. 3–60.

[2] M. Geetha, A.K. Singh, R. Asokamani, A.K. Gogia, Ti based biomaterials, the ultimate choice for orthopaedic implants-A review, Prog. Mater. Sci. 54 (2009) 397–425.

[3] W. Xu, J.J. Tian, Z. Liu, X. Lu, M.D. Hayat, C. Huang, X.H. Qu, C.E. Wen, Novel porous Ti35Zr28Nb scaffolds fabricated by powder metallurgy with excellent osteointegration ability for bone-tissue engineering applications, Mater. Sci. Eng. C 105 (2019) 110015.

[4] H. Kröger, P. Venesmaa, J. Jurvelin, H. Miettinen, O. Suomalainen, E. Alhava, Bone density at the proximal femur after total hip arthroplasty, Clin. Orthop. Relat. Res. 352 (1998) 66–74.

[5] B. Aksakal, O.S. Yildirim, H. Gul, Metallurgical failure analysis of various implant materials used in orthopedic applications, J. Fail. Anal. Prev. 4 (2004) 17–23.

[6] W. Xu, X. Lu, J.J. Tian, C. Huang, M.o Chen, Y. Yan, L.N. Wang, X.H. Qu, C.E. Wen, Microstructure, wear resistance, and corrosion performance of Ti35Zr28Nb alloy fabricated by powder metallurgy for orthopedic applications, J. Mater. Sci. Technol. 41 (2020) 191–198.

[7] W. Xu, X. Lu, M.D. Hayat, J.J. Tian, C. Huang, M. Chen, X.H. Qu, C.E. Wen, Fabrication and properties of newly developed Ti35Zr28Nb scaffolds fabricated by powder metallurgy for bone-tissue engineering, J. Mater. Res. Technol. 8 (2019) 3696–3704.

[8] W. Xu, X. Lu, L.N. Wang, Z.M. Shi, S.M. Lv, Q. Ma, X.H. Qu, Mechanical properties, in vitro corrosion resistance and biocompatibility of metal injection molded Ti-12Mo alloy for dental applications, J. Mech. Behav. Biomed. 88 (2018) 534–547.

[9] W. Xu, M. Chen, X. Lu, D.W. Zhang, H.P. Singh, J.S. Yu, Y. Pan, X.H. Qu, C.Z. Liu, Effect of Mo content on corrosion and tribocorrosion behaviours of Ti-Mo orthopaedic alloys fabricated by powder metallurgy, Corrosion Sci. (2020) 108557.

[10] W.F. Ho, C.P. Ju, J.C. Lin, Structure and properties of cast binary Ti-Mo alloys, Biomaterials 20 (1999) 2115–2122.

[11] W. Xu, Z. Liu, X. Lu, J.J. Tian, G. Chen, B.W. Liu, Z. Li, X.H. Qu, C.E. Wen, Porous Ti-10Mo alloy fabricated by powder metallurgy for promoting bone regeneration, Sci. China Mater. 62 (2019) 1053–1064.

[12] N.T.C. Oliveira, A.C. Guastaldi, Electrochemical stability and corrosion resistance of Ti-Mo alloys for biomedical applications, Acta Biomater. 5 (2009) 399–405.

[13] W. Xu, X. Lu, B. Zhang, C.C. Liu, S.M. Lv, S.D. Yang, X.H. Qu, Effects of porosity on mechanical properties and corrosion resistance of PM-fabricated porous Ti-10Mo alloy, Metals 8 (2018) 188–201.

[14] V.R. Jablokov, M.J. Nutt, M.E. Richelsoph, H.L. Freese, The application of Ti-15Mo beta titanium alloy in high strength structural orthopaedic applications, J. ASTM Int. (JAI) 2 (2005) 1–8.

[15] J. Disegi, Wrought Titanium-15% Molybdenum Implant Material, SYNTHES® Instruments and Implants, second ed., (April 2009).

[16] P.J. Bania, Beta titanium alloys and their role in the titanium industry, J. Occup. Med. 46 (1994) 16–19.

[17] G. De Bastiani, R. Aldegheri, L. Renzi Brivio, The treatment of fractures with a dynamic axial fixator, J. Bone Joint Surg. 66 (1984) 538–545.

[18] M. Deysine, Infections associated with surgical implants, N. Engl. J. Med. 351 (2004) 193–195.

[19] Y.Z. Wan, G.Y. Xiong, H. Liang, S. Raman, F. He, Y. Huang, Modification of medical metals by ion implantation of copper, Appl. Surf. Sci. 253 (2007) 9426–9429.

[20] M. Yoshinari, Y. Oda, T. Kato, K. Okuda, Influence of surface modifications to titanium on bacterial inhibitory activity in vitro, Biomaterials 22 (2001) 2043–2048.

[21] X. Wang, H. Dong, J. Liu, G. Qin, D. Chen, E. Zhang, In vivo bacterial inhibitory property of Ti-Cu sintered alloy implant, Mater. Sci. Eng. C 100 (2019) 38–47.

[22] B. Szaraniec, T. Goryczka, Structure, and properties of Ti-Ag alloys produced by powder metallurgy, J. Alloys Compd. 709 (2017) 464–472.

[23] L. Zhang, J. Guo, T. Yan, Y. Han, Fibroblast responses and bacterial inhibitory activity of Cu and Zn co-doped $TiO_2$ for percutaneous implants, Appl. Surf. Sci. 434 (2018) 633–642.

[24] F. Heidenau, W. Mittelmeier, R. Detsch, M. Haenle, F. Stenzel, G. Ziegler, H. Gollwitzer, A novel bacterial inhibitory titania coating: metal ion toxicity and in vitro surface colonization, J. Mater. Sci. 16 (2005) 883–888.

[25] L. Ren, H.M. Wong, C.H. Yan, Kelvin W.K. Yeung, K. Yang, Osteogenic ability of Cu-bearing stainless steel, J. Biomed. Mater. Res. Part B 103B (2015) 1433–1444.

[26] K. Glenske, P. Donkiewicz, A. Köwitsch, N. Milosevic-Oljaca, P. Rider, S. Rofall, J. Franke, O. Jung, R. Smeets, R. Schnettler, S. Wenisch, M. Barbeck, Applications of metals for bone regeneration, Int. J. Mol. Sci. 19 (2018) 826–858.

[27] H. Chai, L. Guo, X. Wang, Y. Fu, J. Guan, L. Tan, L. Ren, K. Yang, Bacterial inhibitory effect of 317L stainless steel contained copper in the prevention of implant-related infection in vitro and in vivo, J. Mater. Sci. Mater. Med. 22 (2011) 2525–2535.

[28] T. Shirai, H. Tsuchiya, T. Shimizu, K. Ohtani, Y. Zen, K. Tomita, Prevention of pin tract infection with titanium-copper alloys, J. Biomed. Mater. Res. B 91B (2009) 373–380.

[29] E.R. Zhang, F. Li, H.Y. Wang, J. Liu, C.M. Wang, M.Q. Li, K. Yang, A new bacterial inhibitory titanium-copper sintered alloy: preparation and bacterial inhibitory property, Mater. Sci. Eng. C 33 (2013) 4280–4287.

[30] L. Ren, Z. Ma, M. Li, Y. Zhang, W.Q. Liu, Z.H. Liao, K. Yang, Bacterial inhibitory properties of Ti-6Al-4V-xCu alloys, J. Mater. Sci. Technol. 30 (2014) 699–705.

[31] W. Xu, M. Li, C.E. Wen, S.M. Lv, C.C. Liu, X. Lu, X.H. Qu, The mechanical properties and in vitro biocompatibility of pm-fabricated Ti-28Nb-35.Zr alloy for orthopedic implant applications, Materials 11 (2018) 531–543.

[32] W. Xu, S.Q. Xiao, X. Lu, G. Chen, C.C. Liu, X.H. Qu, Fabrication of commercial pure Ti by selective laser melting using hydride-dehydride titanium powders treated by ball milling, J. Mater. Sci. Technol. 35 (2019) 322–327.

[33] ASTM B962-14, Standard Test Methods for Density of Compacted or Sintered Powder Metallurgy (PM) Products Using Archimedes' Principle, ASTM International, West Conshohocken, PA, 2017.

[34] ISO 10993-5, Biological Evaluation of Medical Devices-Part 5: Tests for Cytotoxicity: in Vitro Methods, ANSI/AAMI, Arlington, VA, 1999.

[35] QB/T 2591, Antimicrobial Plastics Test for Antimicrobial Activity and Efficacy, (2003).

[36] K.N. Campo, E.S.N. Lopes, C.J. Parrish, R. Caram, Rapid quenching of semisolid Ti-Cu alloys: insights into globular microstructure formation and coarsening, Acta Mater. 139 (2017) 86–95.

[37] Z. Ma, M. Li, R. Liu, L. Ren, Y. Zhang, H.B. Pan, Y. Zhao, K. Yang, In vitro study on an bacterial inhibitory Ti–5Cu alloy for medical application, J. Mater. Sci. Mater. Med. 27 (2016) 91–103.

[38] T. Aoki, I.C.I. Okafor, I. Watanabe, M. Hattori, Y. Oda, T. Okabe, Mechanical properties of cast Ti-6Al-4V-XCu alloys, J. Oral Rehabil. 31 (2011) 1109–1114.

[39] J.W. Wang, S.y. Zhang, Z.Q. Sun, H. Wang, L. Ren, K. Yang, Optimization of mechanical property, bacterial inhibitory property and corrosion resistance of Ti-Cu alloy for dental implant, J. Mater. Sci. Technol. 35 (2019) 2336–2344.

[40] E.L. Zhang, J. Ren, S.Y. Li, L. Yang, G.W. Qin, Optimization of mechanical properties, biocorrosion properties and antibacterial properties of as-cast Ti-Cu alloys, Biomed. Mater. 11 (2016) 065001.

[41] Z. Ma, M. Yao, R. Liu, K. Yang, L. Ren, Y. Zhang, Z. Liao, W. Liu, M. Qi, Study on bacterial inhibitory activity and cytocompatibility of Ti-6Al-4V-5Cu alloy, Mater. Technol. 30 (sup6) (2015) B80–B85.

[42] J. Liu, X.X. Zhang, H.Y. Wang, F.B. Li, M.Q. Li, K. Yang, E.L. Zhang, The bacterial inhibitory properties and biocompatibility of a Ti-Cu sintered alloy for biomedical application, Biomed. Mater. 9 (2014) 025013.